Simultaneous whole-liver water T1 and T2 mapping with isotropic resolution during free-breathing

Supplementary information

	T2-weighted	**Post-contrast T1-weighted**	**Dixon quant (for PDFF mapping)**
Motion compensation	Triggered	Breath-hold	Breath-hold
Voxel size (mm^3)	1.3×1.3×4 (2D)	1.5×1.62×5 (3D)	2×3×6 (3D)
FOV (mm^3)	pat #1: 430×430×264 pat #3: 400×400×264	pat #1: 450×400×262 pat #3: 400×318×262	300×400×150
TE (ms)	pat #1: 151 pat #3: 126	1.31/2.3	TE_1=1.35, ΔTE=1.1
TR (ms)	pat #1: 2160 pat #3: 2172	3.6	7.84
FA (°)	90	10	3
Acceleration	SENSE (R=2.5)	CS-SENSE (R=6)	CS-SENSE (R=4)
Scan time (min:s)	3:36 (nominal)	00:12	00:09

Table S1: Sequence parameters for the institutional conventional clinical liver protocol. Some sequence parameters differ between patient #1 and #3 due to their body size.

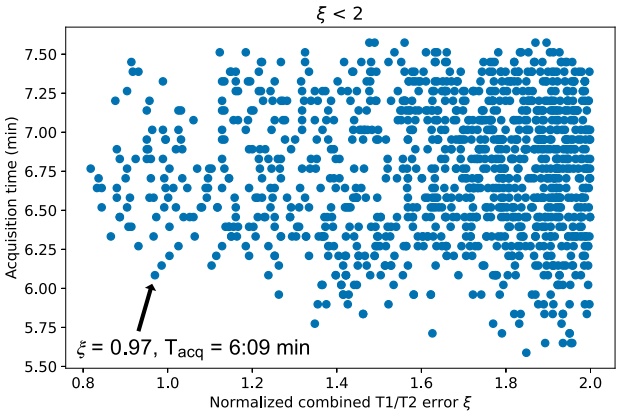

Figure S1: Optimization of delay and waiting time for the proposed wT1 and wT2 mapping technique. Sequence parameters were selected to minimize both the combined T1 and T2 mapping error (ξ) and acquisition time. The optimal parameter set, consisting of T_{delay} and T_{wait}, was determined through visual analysis of this plot (highlighted by the black arrow).

Vial	PDFF (%)	Proposed wT1	MOLLI T1	STEAM TI wT1	SHORTIE wT1
1.1	0	482.7 ± 5.8	479.8 ± 4.2	491.7	489.5
1.2	0	671.6 ± 15.7	678.2 ± 6.7	698.3	690.2
1.3	0	893.6 ± 46.9	888.7 ± 6.2	915.9	908.9
1.4	0	1129.2 ± 84.0	1093.0 ± 11.7	1113.9	1109.4
1.5	4.9	472.4 ± 6.4	487.2 ± 4.3	486.0	483.2
1.6	5.2	671.7 ± 17.1	700.2 ± 4.8	696.6	689.6
1.7	5.5	909.6 ± 48.9	931.1 ± 8.2	914.6	910.6
1.8	5.5	1148.8 ± 72.3	1154.6 ± 13.4	1119.7	1111.6
1.9	9.9	482.1 ± 7.2	509.0 ± 10.0	493.5	490.6
1.10	10.0	674.7 ± 12.8	734.8 ± 7.5	697.2	689.0
1.11	10.9	964.5 ± 48.9	994.0 ± 12.4	917.4	906.8
1.12	11.0	1259.9 ± 91.8	1254.1 ± 17.4	1133.4	1121.2
2.1	0	659.6 ± 19.8	634.4 ± 5.6	684.1	664.1
2.2	0	132.4 ± 8.5	374.7 ± 18.8	125.8	131.8
2.3	0	313.5 ± 7.4	259.6 ± 54.5	303.0	303.7
2.4	0	1575.1 ± 138.5	1650.1 ± 13.8	1585.0	1551.2
2.5	0	158.1 ± 10.3	271.2 ± 12.0	157.5	163.6
2.6	32.0	253.6 ± 10.4	224.4 ± 17.5	222.2	226.0

Table S2: Summary of the wT1 mapping results in both phantoms: T1 Calimetrix phantom and T2 custom-built phantom. Results are denoted in ms.

Vial	PDFF (%)	Proposed wT2	Dixon Spin Echo wT2	GRASE T2	PRESS wT2
1.1	0	65.5 ± 2.0	59.8 ± 1.3	69.5 ± 1.1	65.4
1.2	0	68.4 ± 2.4	63.9 ± 1.9	74.6 ± 1.5	67.4
1.3	0	70.0 ± 2.8	65.7 ± 2.3	77.5 ± 1.4	68.7
1.4	0	71.1 ± 2.3	69.2 ± 2.6	76.9 ± 1.9	70.2
1.5	4.9	62.6 ± 2.6	58.6 ± 1.3	69.7 ± 1.8	59.8
1.6	5.2	62.6 ± 1.7	59.8 ± 1.7	74.0 ± 1.4	59.2
1.7	5.5	63.3 ± 1.6	61.2 ± 2.1	75.2 ± 1.6	59.7
1.8	5.5	64.0 ± 2.0	62.7 ± 2.3	72.1 ± 1.8	60.0
1.9	9.9	58.6 ± 2.6	56.0 ± 1.7	70.2 ± 1.6	54.6
1.10	10.0	58.1 ± 1.9	57.4 ± 1.9	72.2 ± 1.3	54.8
1.11	10.9	60.5 ± 1.8	58.5 ± 2.3	74.3 ± 1.7	54.4
1.12	11.0	60.0 ± 1.7	59.1 ± 2.5	70.8 ± 1.7	54.0
2.1	0	30.2 ± 1.4	30.5 ± 0.5	33.7 ± 2.5	30.6
2.2	0	12.1 ± 0.8	10.0 ± 0.3	12.3 ± 3.0	11.1
2.3	0	19.9 ± 0.9	19.5 ± 0.3	21.6 ± 2.4	19.5
2.4	0	38.5 ± 2.6	35.8 ± 1.3	45.3 ± 2.8	39.9
2.5	0	15.3 ± 1.2	12.2 ± 0.3	14.1 ± 2.6	12.9
2.6	32.0	13.2 ± 1.1	13.4 ± 0.5	37.8 ± 3.6	12.6

Table S3: Summary of the wT2 mapping results in both phantoms (T1 and T2 phantoms). Results are denoted in ms.

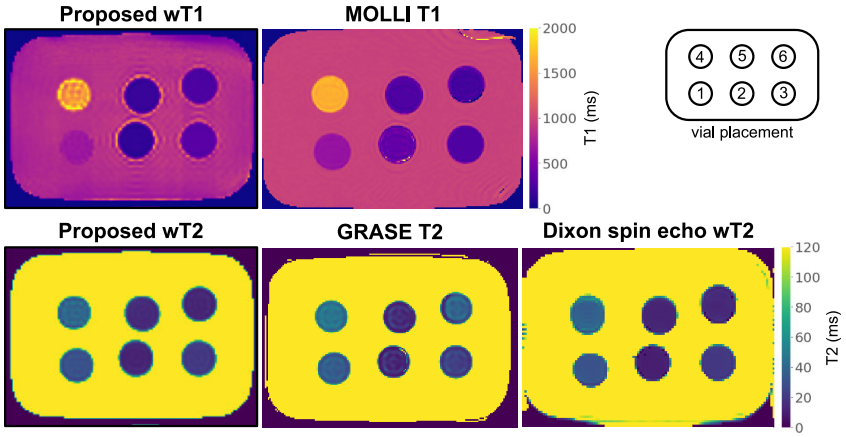

Figure S2: Comparison of the proposed water-specific T1 and T2 mapping with conventional methods (MOLLI T1, GRASE T2 and Dixon spin echo wT2) for the custom-built T2 phantom.

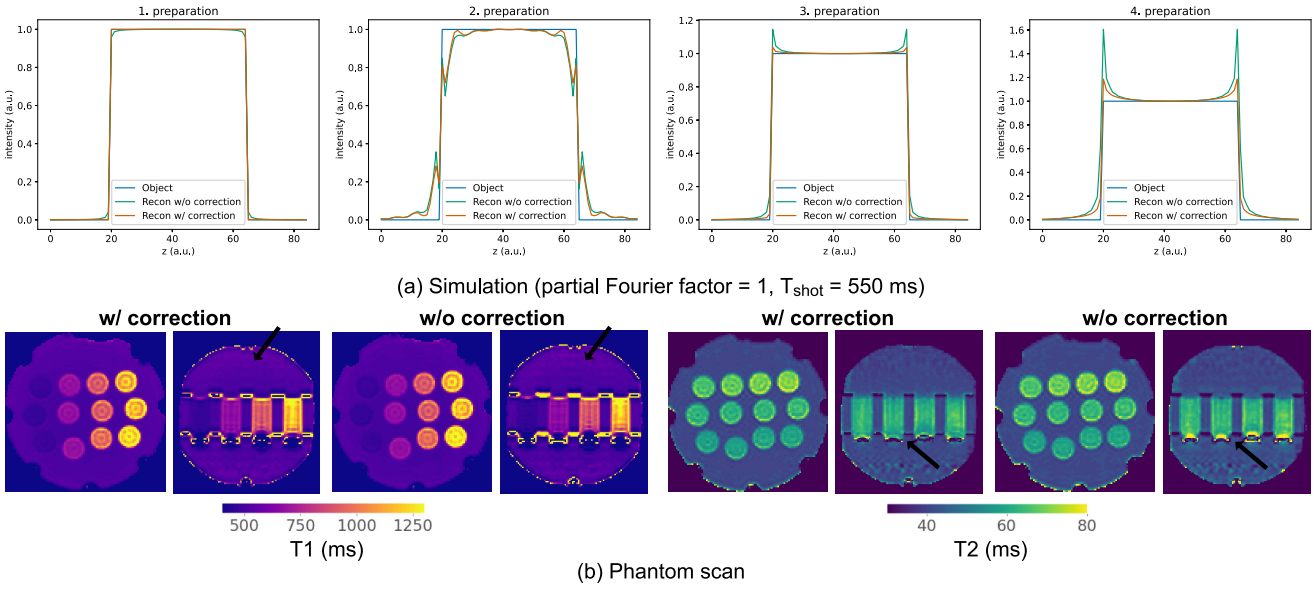

Figure S3: Assessing the importance of the implemented T1 blurring correction using k-space weighting. (a) The k-space of a rectangular object (T1=800 ms, T2=30 ms) was simulated with T1 relaxation blurring based on Bloch simulation, with increased shot duration for a simplified acquisition without partial Fourier sampling. Reconstructions with (orange) and without (green) the proposed T1 blurring correction are compared. (b) Phantom scan reconstructions with and without the suggested relaxation blurring correction. The arrows show differences between the two reconstructions. There is considerably less ringing in the images along the slice dimension with the proposed correction (black arrow in the T1 map).

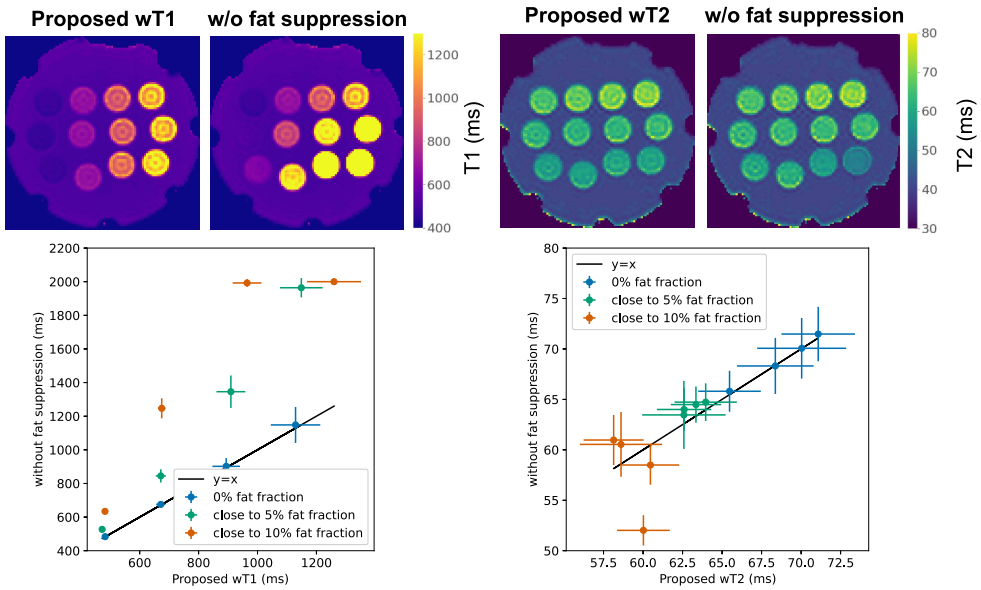

Figure S4: Demonstration of the importance of fat suppression for dictionary matching. To evaluate the effect of fat on T1 and T2 mapping, dictionary matching was performed on the first echo image containing water and fat species with distinct relaxation properties. Phantom maps are shown on the top, while a quantitative evaluation, separated by fat fraction, is presented on the bottom.

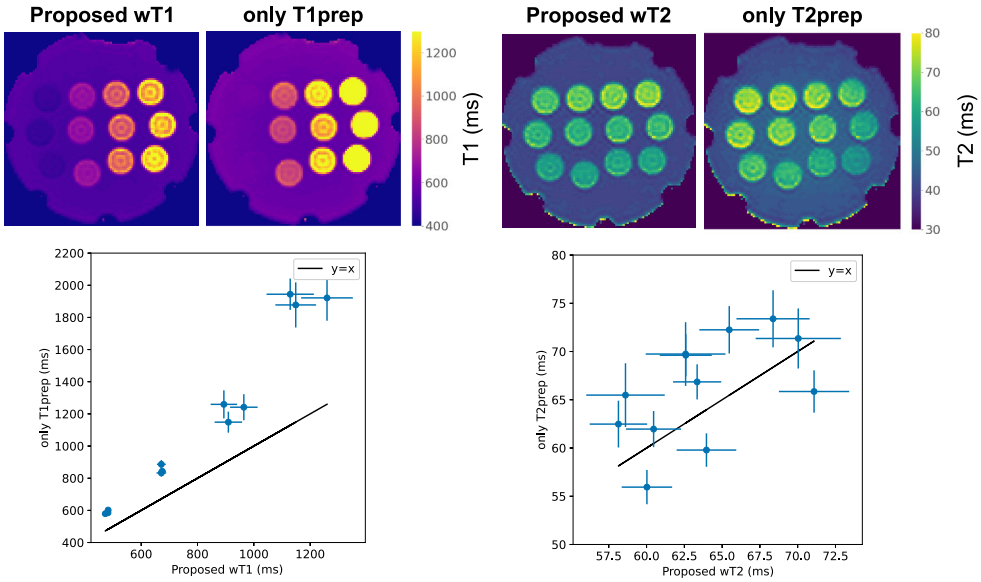

Figure S5: Demonstration of the importance of simultaneous T1 and T2 mapping for dictionary matching. To assess the impact of simultaneous relaxation parameter mapping, dictionary matching was performed with only T1 preparations or T2 preparations, fixing the other parameter (T2=30 ms for T1prep and T1=800 ms for T2prep). Phantom maps are shown on the top, while a quantitative evaluation is presented on the bottom.

#	Proposed wT1	Proposed wT2	SHORTIE wT1	GRASE T2	PRESS wT2
1	882.5 ± 140.2	33.0 ± 3.7	819.8	51.6 ± 4.1	40.1
1	828.6 ± 50.1	36.0 ± 2.6	799.8	48.5 ± 3.0	40.7
1	858.2 ± 76.7	37.1 ± 1.9	827.0	54.1 ± 9.0	41.8
2	877.9 ± 310.9	27.7 ± 4.6	765.9	50.0 ± 12.5	30.9
2	782.0 ± 80.2	28.2 ± 3.3	710.4	45.1 ± 6.2	34.8
2	689.9 ± 80.6	32.0 ± 4.5	767.8	37.4 ± 3.7	29.6
3	946.0 ± 160.2	29.2 ± 2.0	793.2	41.7 ± 8.4	32.9
3	821.5 ± 63.2	32.7 ± 2.3	790.9	44.4 ± 5.3	26.8
3	828.9 ± 130.4	30.7 ± 2.7	786.1	48.9 ± 5.0	29.0
4	939.0 ± 93.3	24.7 ± 2.0	712.8	36.7 ± 4.5	27.2
4	907.5 ± 45.6	28.0 ± 1.2	755.1	42.4 ± 4.0	24.1
4	906.1 ± 85.1	27.1 ± 2.3	790.0	39.2 ± 5.8	25.3
5	826.6 ± 30.9	27.7 ± 1.1	734.1	36.7 ± 3.7	28.0
5	766.0 ± 60.3	29.0 ± 1.6	756.6	43.1 ± 7.8	29.4
5	780.3 ± 64.9	29.5 ± 1.5	785.3	42.7 ± 8.7	32.0
6	795.3 ± 74.3	24.2 ± 1.5	691.4	40.3 ± 4.0	26.8
6	727.3 ± 60.4	23.9 ± 2.3	709.8	44.3 ± 6.7	25.5
6	725.8 ± 62.3	23.5 ± 1.7	720.5	43.5 ± 5.4	26.4
7	830.8 ± 58.3	26.6 ± 1.2	699.0	42.7 ± 4.9	31.5
7	814.3 ± 44.3	26.5 ± 0.9	738.7	41.5 ± 4.5	31.3
7	829.7 ± 108.4	27.2 ± 2.9	779.1	46.5 ± 12.1	34.8
8	760.9 ± 111.6	26.5 ± 2.8	706.2	33.0 ± 7.6	25.1
8	889.8 ± 276.5	27.7 ± 3.5	728.1	53.2 ± 16.7	36.1
8	760.4 ± 55.9	24.3 ± 1.8	743.3	40.0 ± 7.5	27.8
9	633.9 ± 72.7	17.9 ± 1.2	654.7	33.0 ± 7.3	26.5
9	677.6 ± 74.9	15.8 ± 1.5	647.0	25.7 ± 5.9	20.1
9	614.6 ± 62.7	18.3 ± 2.4	657.9	30.2 ± 10.9	21.5
10	859.2 ± 58.2	29.0 ± 2.0	751.4	41.5 ± 3.7	31.5
10	822.8 ± 50.4	29.4 ± 1.9	755.6	41.8 ± 5.4	29.2
10	804.1 ± 89.8	29.7 ± 1.8	735.8	42.6 ± 5.3	31.8

Table S4: Summary of the spectroscopy results (SHORTIE wT1 and PRESS wT2) in the volunteer study. Results were compared to the proposed wT1 and wT2 mapping and GRASE T2 mapping based on the position of the spectroscopy voxels. Results are denoted in ms.

	First scan			Second scan	
#	MOLLI T1	Proposed wT1	Proposed wT2	Proposed wT1	Proposed wT2
1	910.8 ± 57.5	924.2 ± 45.0	33.9 ± 1.0		
1	947.0 ± 47.4	863.9 ± 31.3	35.5 ± 2.8		
1 (Muscle)	1109.1 ± 25.1	978.3 ± 58.6	26.9 ± 1.0		
2	785.8 ± 51.7	737.5 ± 38.5	27.0 ± 1.6		
2	763.7 ± 26.1	692.1 ± 72.1	29.4 ± 3.1		
2 (Muscle)	1120.8 ± 22.1	1165.8 ± 136.7	27.9 ± 1.5		
3	812.9 ± 19.8	781.7 ± 23.3	30.7 ± 0.9	805.0 ± 17.6	32.8 ± 0.9
3	835.6 ± 43.3	830.4 ± 72.6	32.2 ± 2.3	865.4 ± 54.6	30.6 ± 1.7
3 (Muscle)	1078.8 ± 21.8	1062.1 ± 90.8	25.3 ± 1.5	982.9 ± 33.2	25.2 ± 0.6
3		774.2 ± 41.8	29.6 ± 0.9	809.6 ± 36.1	31.5 ± 0.8
3		832.9 ± 28.6	30.0 ± 0.9	813.8 ± 21.0	33.6 ± 1.2
3		951.3 ± 55.4	28.5 ± 1.1	922.1 ± 46.6	29.4 ± 1.3
4	851.3 ± 65.8	966.3 ± 70.8	25.0 ± 2.4		
4	864.9 ± 76.6	920.8 ± 36.7	29.0 ± 1.1		
4 (Muscle)	1133.0 ±30.6	1100.0 ± 70.0	25.3 ± 1.2		
5	882.9 ± 69.0	784.6 ± 53.6	29.3 ± 1.2	715.8 ± 28.5	28.8 ± 1.5
5	850.2 ± 70.5	812.9 ± 22.4	28.2 ± 0.9	768.8 ± 24.9	28.9 ± 1.1
5 (Muscle)	1193.6 ± 39.8	1027.5 ± 107.2	27.5 ± 1.3	1021.3 ± 85.6	27.2 ± 1.0
5		836.7 ± 36.6	28.0 ± 1.3	795.4 ± 23.2	27.3 ± 0.8
5		755.4 ± 47.2	29.0 ± 1.2	800.8 ± 36.0	27.9 ± 1.1
5		746.3 ± 47.3	29.5 ± 1.1	802.1 ± 27.1	29.1 ± 1.0
6	755.9 ± 39.6	760.8 ± 29.6	24.2 ± 1.0	771.3 ± 37.7	23.6 ± 1.2
6	781.9 ± 40.4	720.0 ± 44.1	23.2 ± 1.0	747.5 ± 42.0	22.8 ± 1.2
6 (Muscle)	1152.0 ± 63.8	1002.5 ± 73.8	27.2 ± 1.0	998.8 ± 54.2	27.0 ± 2.0
6		711.7 ± 29.3	25.3 ± 0.9	775.0 ± 38.1	23.5 ± 0.8
6		714.6 ± 70.5	24.6 ± 2.0	784.2 ± 93.1	24.0 ± 1.7
6		708.3 ± 43.7	23.8 ± 1.2	795.4 ± 86.2	23.3 ± 2.0
7	808.3 ± 53.0	834.2 ± 29.3	27.5 ± 0.7	793.3 ± 27.9	28.3 ± 1.1
7	849.9 ± 67.5	818.3 ± 48.0	29.1 ± 1.3	847.1 ± 48.5	26.9 ± 1.3
7 (Muscle)	1169.8 ± 39.0	1055.8 ± 174.2	28.5 ± 1.2	1100.4 ± 54.1	26.1 ± 1.4
7		774.2 ± 41.8	28.1 ± 1.0	778.3 ± 35.0	28.0 ± 0.9
7		760.4 ± 27.3	27.3 ± 1.1	745.8 ± 39.2	26.5 ± 0.7
7		712.5 ± 42.2	28.5 ± 1.8	764.2 ± 93.3	28.1 ± 2.1
8	809.6 ± 56.0	707.5 ± 32.4	24.7 ± 0.8	769.6 ± 42.2	25.3 ± 0.6
8	786.6 ± 55.8	709.6 ± 29.5	27.5 ± 0.8	681.7 ± 17.5	27.5 ± 1.1
8 (Muscle)	1134.5 ± 128.4	922.1 ± 90.4	25.2 ± 2.0	825.0 ± 80.5	27.5 ± 2.1
8		738.8 ± 26.4	28.4 ± 0.5	791.3 ± 33.3	26.2 ± 1.1
8		688.8 ± 16.6	25.6 ± 0.3	769.6 ± 13.6	25.6 ± 0.3
8		710.0 ± 16.4	25.3 ± 0.8	751.3 ± 21.6	23.9 ± 0.3
9	650.9 ± 80.0	626.7 ± 42.5	16.5 ± 1.0		
9	654.0 ± 71.5	573.8 ± 70.9	18.4 ± 1.8		
9 (Muscle)	1109.4 ± 30.5	965.4 ± 72.0	30.0 ± 1.7		
10	835.0 ± 31.8	924.6 ± 54.9	27.4 ± 1.1		
10	862.2 ± 29.1	767.5 ± 45.6	32.0 ± 2.5		
10 (Muscle)	1153.0 ± 45.9	972.9 ± 72.4	24.2 ± 0.9		

Table S5: Comparison of MOLLI T1 and the proposed wT1 mapping and repeatability results for manually placed ROIs throughout the whole liver. MOLLI T1 is a single-slice technique and values could not be estimated for some of the ROIs used in the repeatability study. Results are denoted in ms.

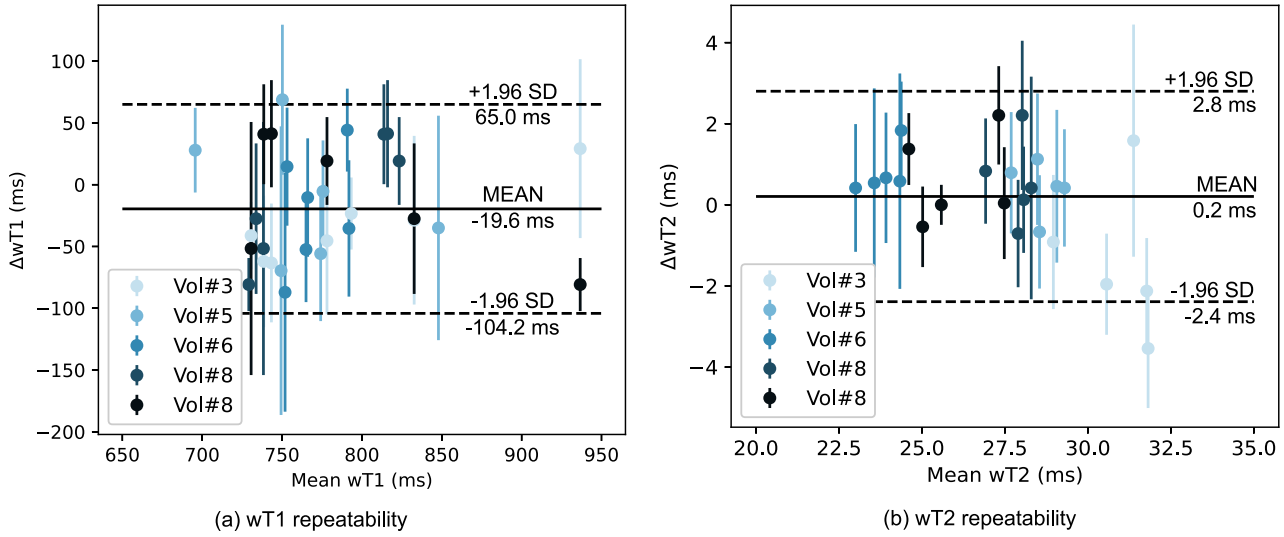

Figure S6: Repeatability analysis of the proposed method in five volunteers. The plot displays the difference between two measurements (vertical axis) and their mean values (horizontal axis), demonstrating excellent repeatability for wT2 and marginally higher values for wT1 in the repeated scan.

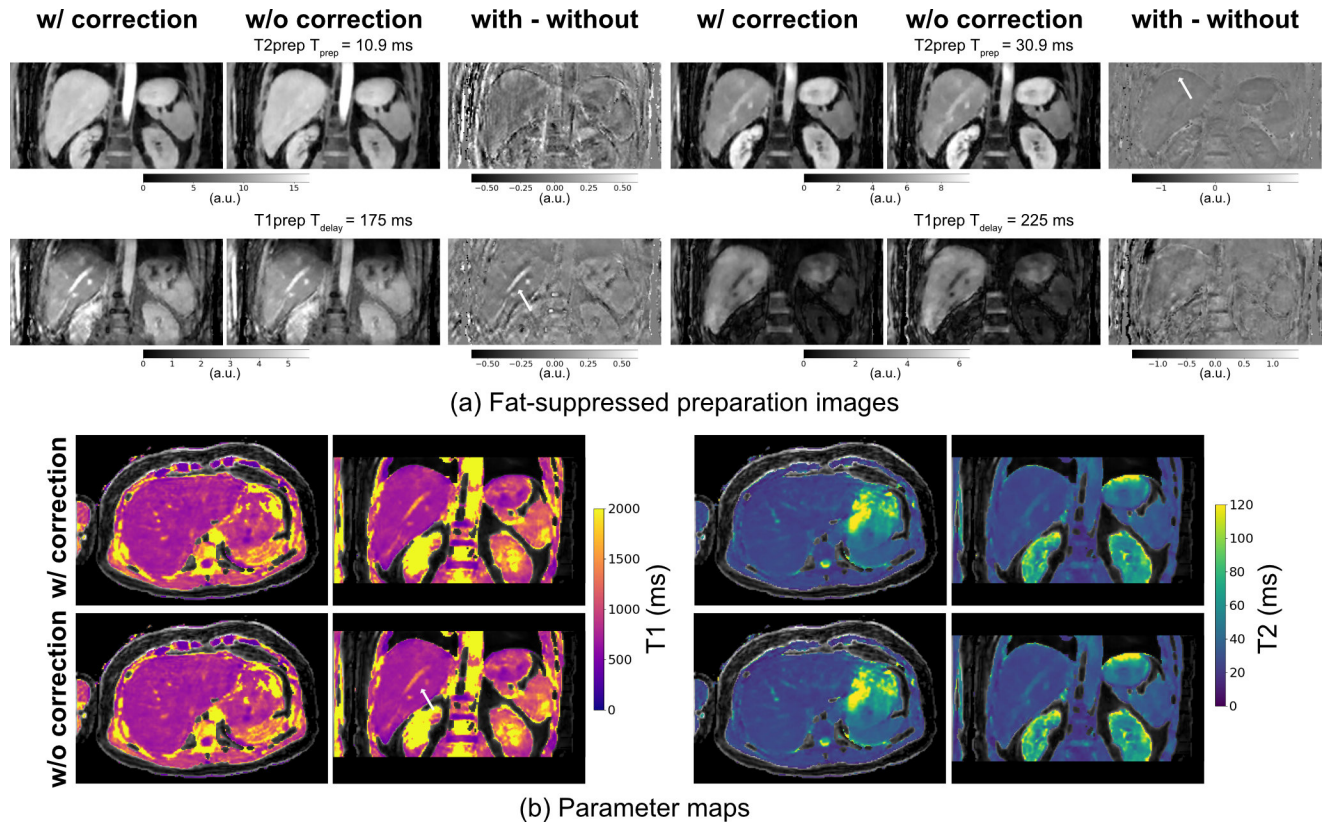

Figure S7: Comparison of the reconstructed fat-suppressed preparation images (a) and parameter maps (b) with and without the proposed T1 blurring correction for volunteer #6. The correction mainly improves the depiction of vessels and interfaces between different tissue (white arrows).

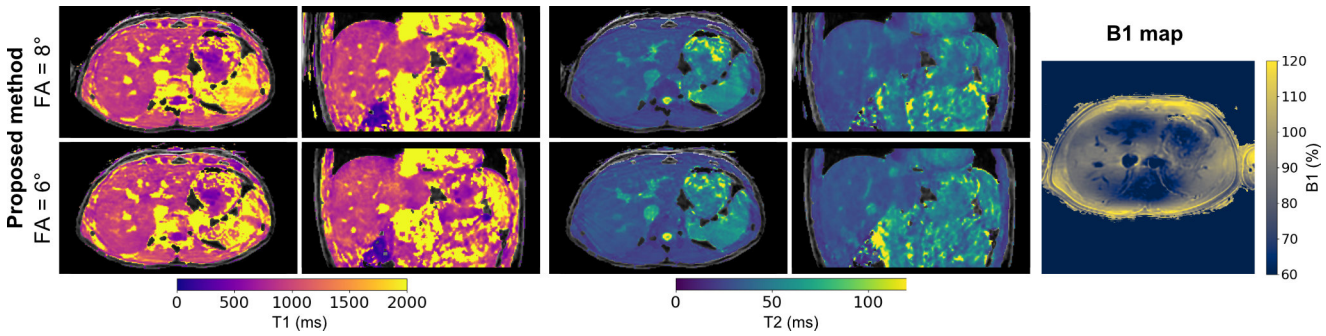

Figure S8: B1 sensitivity evaluation in a volunteer. The proposed method was acquired twice with two different flip angles for the gradient echo readout. The same dictionary was employed for both scans, simulating a reduced B1 of 75% for the scan with FA = 6°. The DREAM B1 map is shown on the right as reference and shows strong B1 inhomogeneities in the range of 60% to 120%. A similar spatial pattern cannot be assessed in the proposed wT1/wT2 maps.

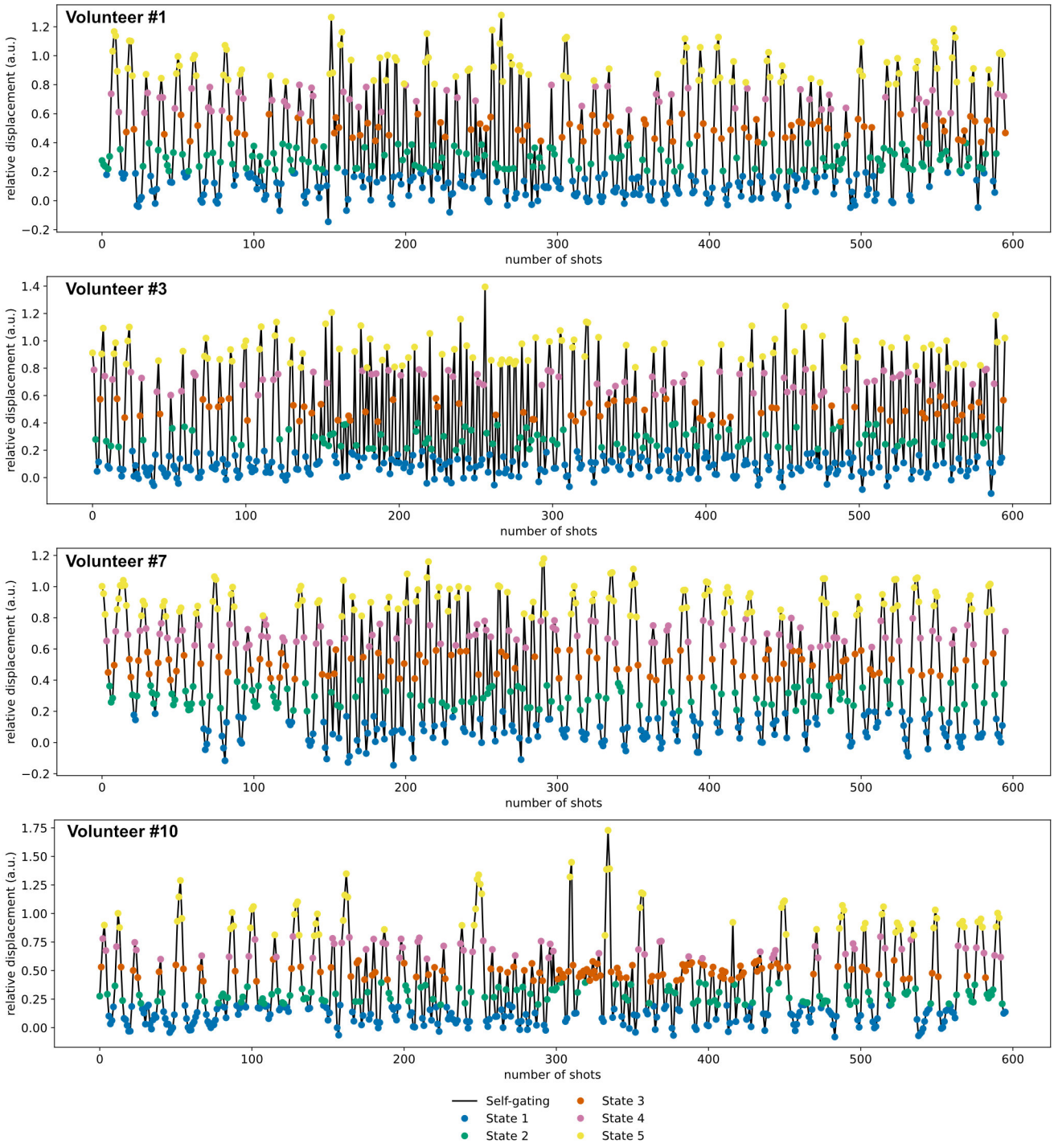

Figure S9: Self-gated respiratory motion signal for volunteer #1, #3, #7 and #10 showing the breathing variability within the volunteer cohort.

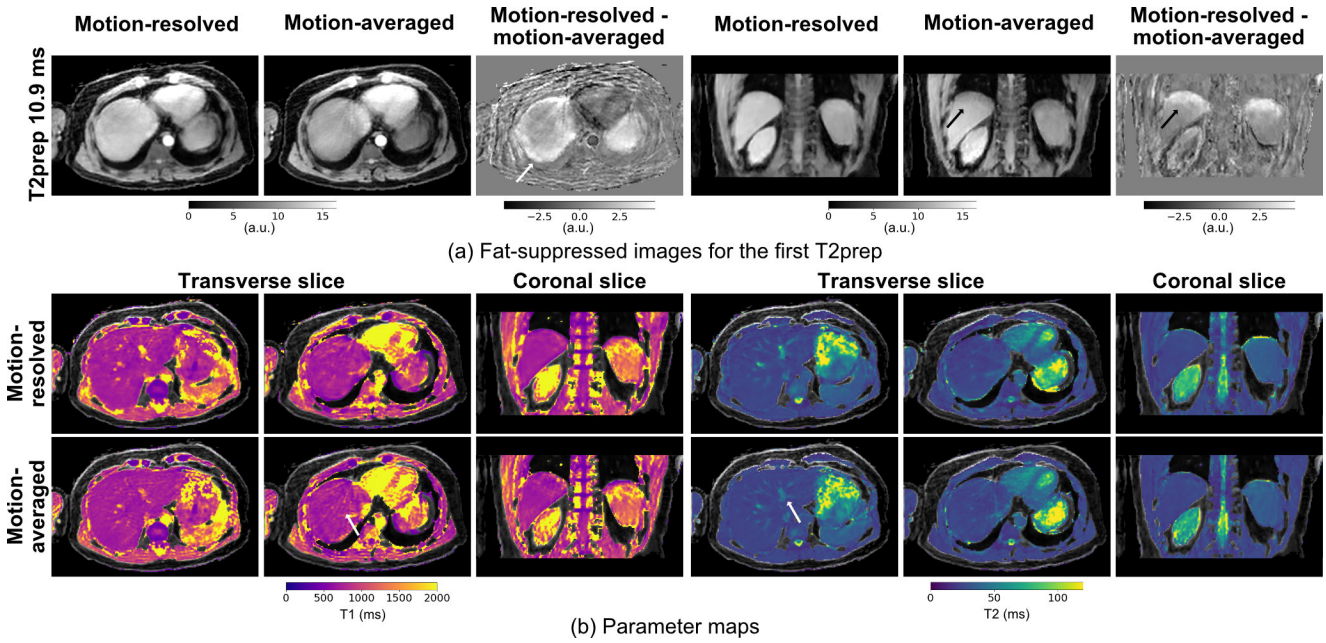

Figure S10: Comparison of the motion-resolved reconstruction results with a motion-averaged reconstruction without any motion correction for volunteer #6. Fat-suppressed images for the first T2prep ($T_{\text{prep}} = 10.9\,\text{ms}$) are show in (a) and parameter maps are shown in (b). The motion-resolved reconstruction improves the visualization of vessels and, in particular, shows less streaking and improved quantification in the upper part of the liver.

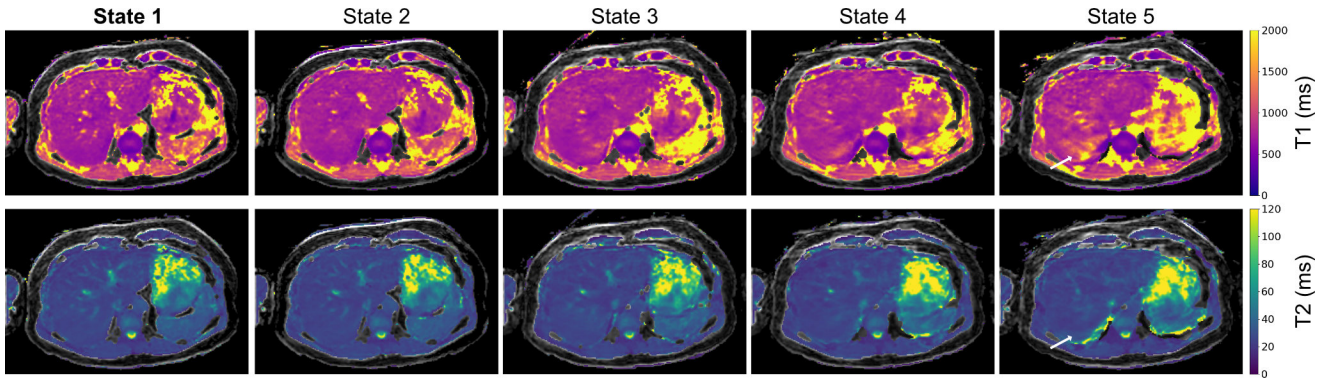

Figure S11: wT1 and wT2 maps for all five motion states, exemplified for volunteer #6. The image quality varies for the motion states, as the number of spokes per motion state varies and depends on the self-navigation signal. Only the first motion state is considered in the study, as the movement information is generally not important for diagnosis.

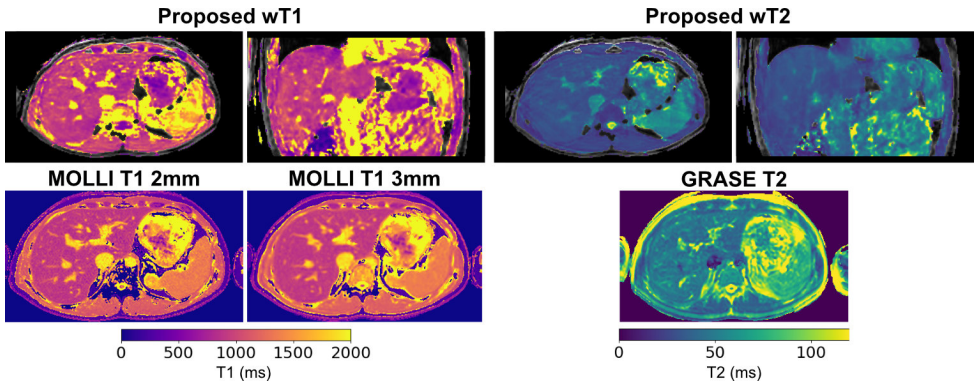

Figure S12: Comparison of the proposed wT1 and wT2 maps with MOLLI T1 and GRASE T2 at the same nominal in-plane spatial resolution in a volunteer. MOLLI T1 was acquired with in-plane resolution of 2 mm (similar to the volunteer study) and 3 mm showing the improved depiction of small details at higher resolution. In comparison with the proposed wT1 maps, the appearance of the vessels is slightly different possibly due to motion.

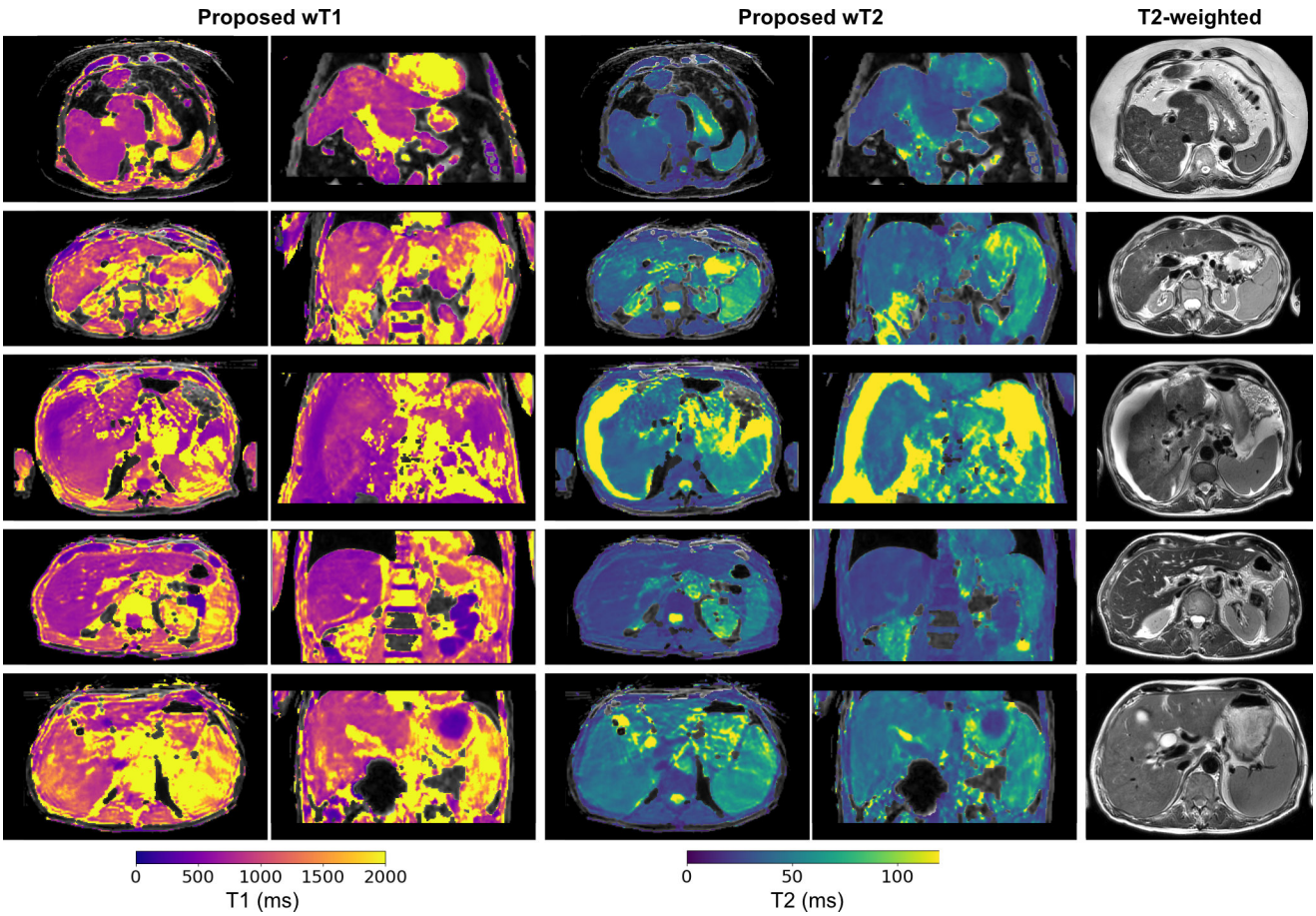

Figure S13: Overview of all patients scanned using the proposed technique. The first (hepatocellular carcinoma and elevated liver fat fraction) and third (liver cirrhosis and ascites) patient are further detailed in Figures 9 and S13. The T1 and T2 mapping results are compared to the T2-weighted sequence used in clinical practice as reference.

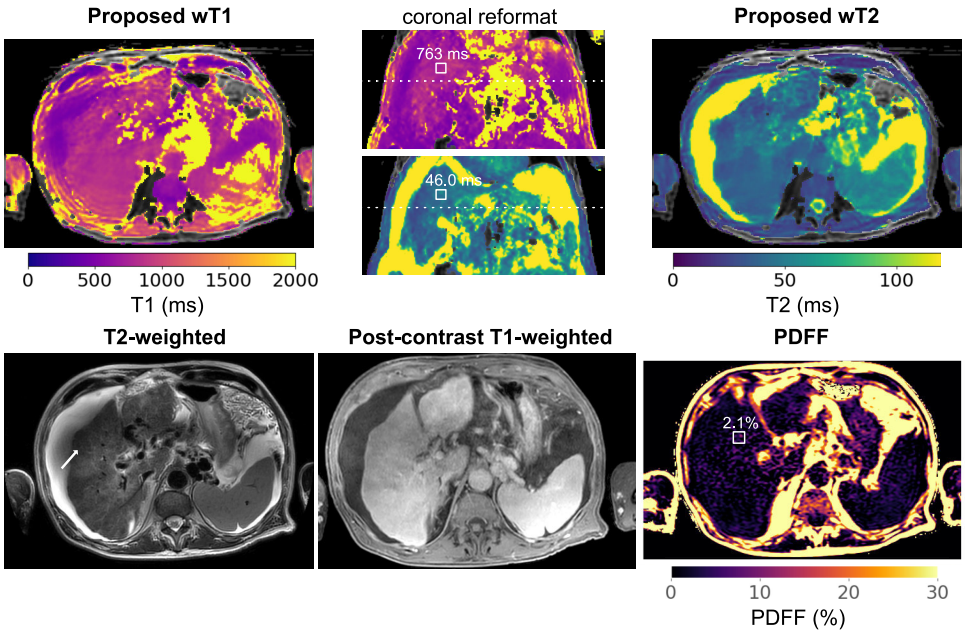

Figure S14: Proposed wT1 and wT2 mapping in patient #3 with liver cirrhosis, exhibiting a nodular liver surface and hypertrophic caudate lobe. The finding of increased T2 may be due to an inflammatory response or edema. Clinically employed T2-weighted sequences, a post-contrast T1-weighted sequence, and the PDFF map are provided as references, indicating fluid accumulation due to ascites. The T2-weighted scan shows shading due to transmit B_1 inhomogeneities next to the fluid (indicated by the arrow). The slice position is illustrated by the dashed line in the coronal reformat of the wT1 and wT2 maps. Mean liver T1 and T2 values are displayed for a ROI in the coronal reformat. Quantification in the fluid may be biased as the sequence is not designed for long T2 values. While the wT1 and wT2 maps are generally homogeneous, some bias can be observed in wT1 and wT2, possibly related to areas that exhibit very severe B_1 inhomogeneities.